TABLE OF CONTENTS

This Page Left Blank Intentionally

SECTION 8

CLOUD PHENOMENA AND CLOUD COVER MODELS

8.1 Introduction. This section presents cloud cover and atmospheric moisture models that can be applied in various NASA mission planning and attenuation studies. There is also a discussion and criteria regarding the high altitude/high latitudinal cloud phenomena existing at stratospheric and mesospheric levels.

A most useful tool in planning experiments and applying space technology to Earth observation is a model of atmospheric parameters. For example, cloud cover data might be used to predict mission feasibility or the probability of observing a given target area in a given number of satellite passes.

To meet the need for atmospheric models, NASA-MSFC sponsored the development of the four-dimensional atmospheric models (8.4) and the worldwide cloud model (8.3). The goal of this work was to produce atmospheric attenuation models to predict degradation effects for all classes of sensors for application to Earth-sensing experiments from spaceborne platforms. To ensure maximum utility and application of these products, NASA-MSFC also sponsored the development of an "Interaction Model of Microwave Energy and Atmospheric Variables," a complete description of the effects of atmospheric moisture upon microwaves (Ref. 8.1).

Cloud related phenomena are presented in other sections of this report such as: precipitation/icing hail/fog in section 7, humidity in section 6, and atmospheric electricity in section 9.

8.2 Interaction Model of Microwave Energy and Atmospheric Variables. While the visible and infrared wavelengths find clouds opaque, the microwave part of the electromagnetic spectrum is unique in that cloud and rain particles vary from very weak absorbers and scatterers to very significant contributors to the electromagnetic environment. This is illustrated in Figures 8.1, 8.2, and 8.3, which are extracted from the final report on the interaction model (Ref. 8.1).

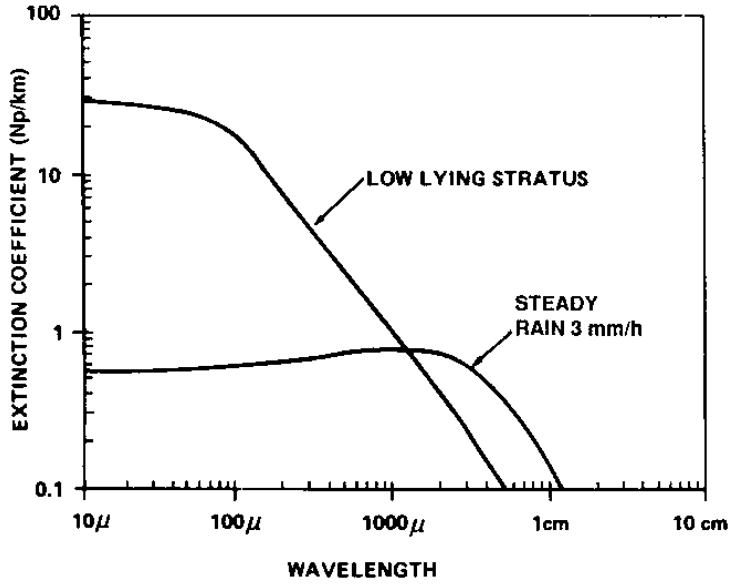

FIGURE 8.1 Extinction Coefficient as a Function of Wavelength.

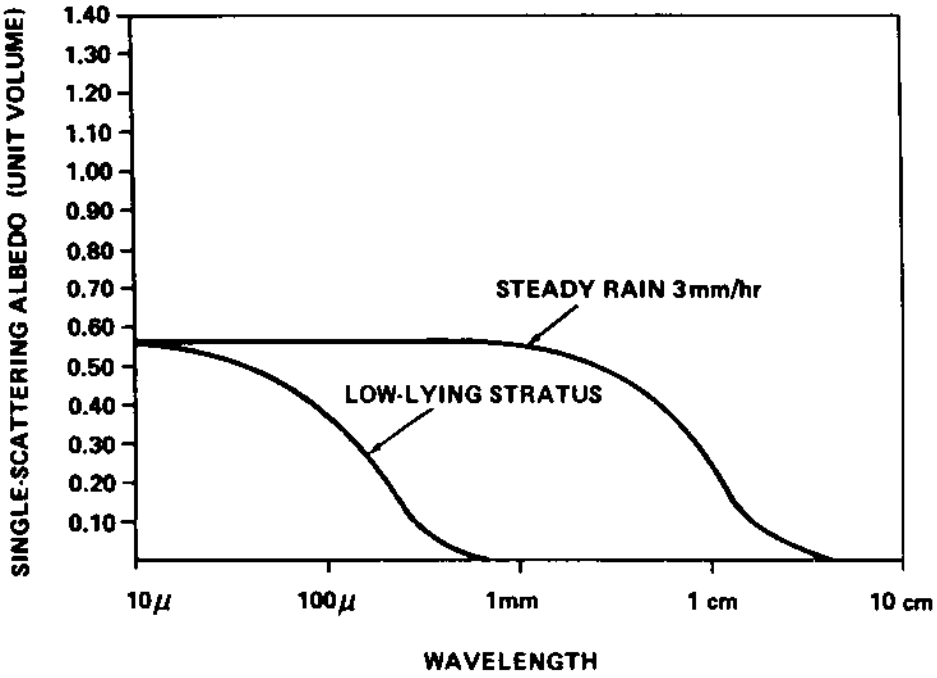

FIGURE 8.2 Single Scattering Albedo for Two Cloud Models.

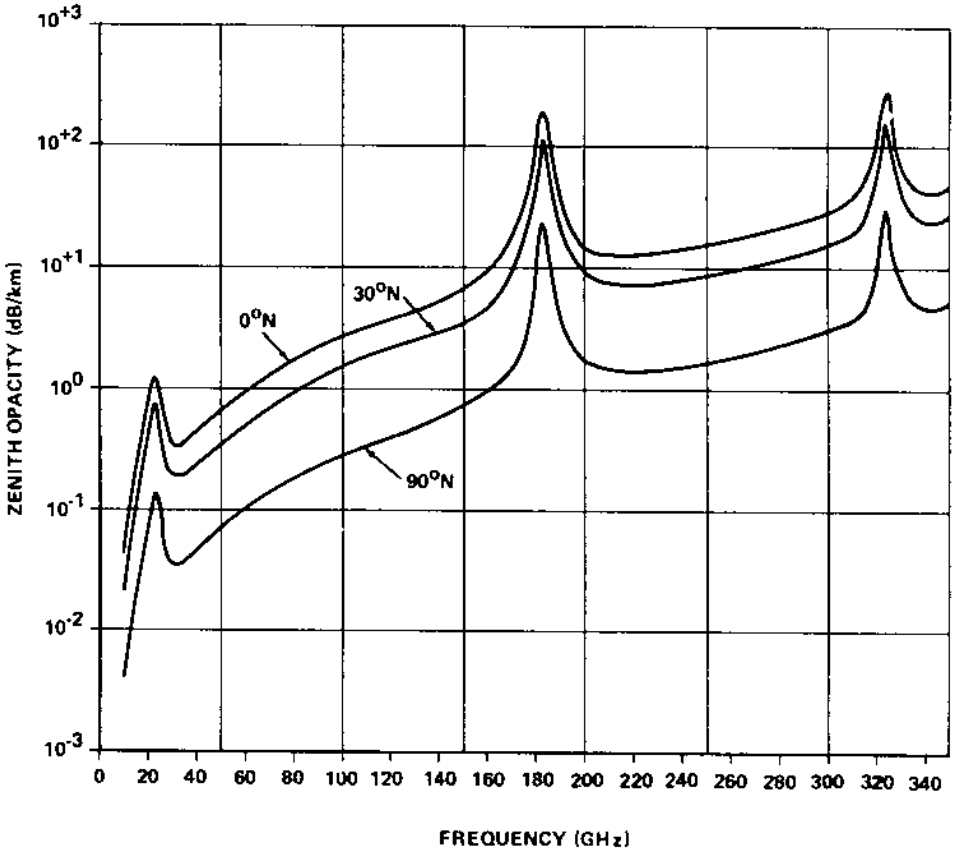

FIGURE 8.3 Zenith Opacity.

8.2.1 Scattering and Extinction Properties of Water Clouds Over the Range 10 cm to 10 μm. Figures 8.1 and 8.2 show the unit-volume scattering and extinction properties of two modeled cloud drop distributions computed using the Mie theory. Figure 8.1 gives the extinction coefficient, in units of Neper (Np), as a function of wavelength. Figure 8.2 presents the single scattering albedo for two cloud models representing low stratus clouds and rainy conditions. The curves show the wavelength regimes appropriate to the two cloud types in which scattering effects are relatively unimportant, and in which the extinction coefficient follows the simple Rayleigh ($1/\lambda^2$) dependence.

8.2.2 Zenith Opacity Due to Atmospheric Water Vapor as a Function of Latitude. In the preparation of figure 8.3, 5 years of climatological data from the MIT Planetary Circulations Project were used to obtain mean water vapor distributions applicable to the latitudes 0° N., 30° N., and 90° N., corresponding to tropical, midlatitude, and arctic conditions. The total water vapor content for the three cases is 4.5, 2.5, and 0.5 g/cm^3, respectively. The curves demonstrate the effect of climatological extremes in simulating and predicting the influence of atmospheric water vapor upon surface observations from a space observer, over the range from 10 to 350 gigahertz. A detailed report on the interaction model (Ref. 8.1) is available upon request to the Earth Science and Applications Division, Space Science Laboratory, NASA/Marshall Space Flight Center.

8.3 Global Cloud Cover Models and Data Bases.

8.3.1 Introduction. When an aircraft or spacecraft is above the tropospheric cloud altitudes, the NASA-MSFC Global Cloud Data Base Model (Ref. 8.6) can be used for Earth observation applications, mission feasibility/planning purposes, or for climate studies. Calculating the probability of viewing a given land target area below, for any given month and time, is possible using this data base. Cloud cover is a key element in the research strategy of the U.S. Climate Program. Cloud information is needed to develop an understanding of the role played by clouds in the radiation balance and to aid in the parameterization of clouds in climate models.

Clouds are also a key factor to be considered in the planning of remote sensing missions of the Earth's surface. Depending upon the extent and thickness of a cloud and upon the wavelengths used by the spaceborne sensor, a cloud has effects on the measured radiation ranging from slight attenuation to total absorption. The complexity of modern sensing systems, with wavelengths in the visible, infrared, and microwave, necessitates detailed information on expected cloud cover to permit intelligent planning and studies. In an earlier recognition of the need for a global cloud data set, the Earth Science and Applications Division at the Marshall Space Flight Center (MSFC) sponsored the development of a global data bank of cloud statistics (Ref. 8.2) and computer techniques to utilize the statistics in various simulation studies (Ref. 8.3). This effort employed only standard ground-based cloud observations.

Concurrent with these studies, MSFC also sponsored the development of another data bank (Refs. 8.4, 8.5). This data bank, known as the four-dimensional (4-D) atmospheric model, contains means and variances of atmospheric pressure, temperature, water vapor, and density from the surface to 25 km above the Earth. Related computer programs were also written to permit the use of this data bank in specifying atmospheric profiles for any latitude, longitude, and month of the year. This 4-D model evolved into the Global Reference Atmosphere Model, 1990 (GRAM-90), as published in reference 8.16.

By using the global cloud cover statistics and the simulation procedure, it was possible to provide an evaluation of the consequence of cloud cover on Earth-viewing space missions or receipt of solar radiation for individual target areas of swaths over small areas.

Although this earlier data set has received extensive use, it has some major limitations. The number of cloud climatic regions was limited by data volume handling capability and by the amount of suitable data available. The entire United States, for example, is effectively covered in only four or five regions. Also, each region is assumed to be completely homogeneous. That is, the base station cloud distribution applies everywhere within that region. The cloud climatologies for nine of the Southern Hemisphere (SH) regions were taken as being seasonal reversals of similar Northern Hemisphere (NH) regions. For some oceanic regions, where representative data could not be obtained, statistics were modified from those of other regions based upon climatological considerations. The satellite-derived data base for the conditional statistics is generally weak. It was necessary to compute conditional probabilities on a seasonal basis to produce an adequate sample size for statistical manipulations. The inconsistency between ground-observed basic or unconditional statistics and satellite-observed conditional distributions has introduced uncertainties in the combined utilization of the two data bases.

The techniques for changing the cloud distributions to make them applicable to larger area sizes, temporal separations other than 24 h, and spatial distances other than 200 nmi, are all theoretical and have not been adequately verified. Finally, the original model is more than 15 years old, and much better data have since been acquired. Consequently, in mid-1981, in an effort to overcome some of these limitations, MSFC sponsored the development of a global cloud cover data base (Ref. 8.6) comprised of one parameter, observed total sky cover, and which became initially available in late 1981.

8.3.2 Background. An extensive investigation revealed no suitable summarized or statistical cloud distributions and only one source of cloud observations that provides global coverage and diurnal variation in a manageable volume. This is the three-dimensional (3-D) NEPH automated cloud analysis prepared by the Air Force Global Weather Center (Refs. 8.7, 8.8). Archived SMS/GOES VISSR data do not provide global coverage and contain eight observations daily from both positions (east and west) only since September 1978 (Ref. 8.9). The polar orbiter satellite data provide global coverage, but only daily hemispheric polar stereographic mosaics are archived (Ref. 8.10). The 3-D NEPH analysis, on the other hand, though possessing some limitations in cloud typing (Ref. 8.11) which are minimized by using total measurements and other known shortcomings (Ref. 8.12) provides the only global coverage of cloud cover amounts at frequent time intervals. These data are directly applicable to mission simulations and for other endeavors.

The 3-D NEPH analysis, a global cloud analysis, is prepared eight times (00Z, 03Z, 06Z, ...) daily by the Air Force Global Weather Central (GWC), Offutt Air Force Base, Nebraska. In the past, it was prepared only four times daily for the SH. The analysis, made from all available cloud data, includes satellite, aircraft, and ground/ship observations. These observations are fitted into a coherent global cloud structure through a scheme that has been fully described by Coburn and by Fye, which largely eliminates the risk of incorporating erroneous data or interpreting snow or sand as clouds. The analysis encompasses 15 altitude layers and includes 22 parameters on a fine mesh grid (approximately 25 nmi spacing at 45° latitude).

The 3-D NEPH analysis has all the attributes required for adequate mission simulations except that it is too voluminous to handle. Fortunately, the data processing at the archiving location reduces the volume to a manageable amount. To further reduce the volume of data, only one parameter - total cloud cover - was selected for the new NASA cloud cover data base, which is described in detail in reference 8.6.

8.3.3 Discussion of Validation. To ensure that the cloud cover amounts in the new NASA cloud cover data base are representative of the real world, several comparisons with ground observed sky cover were made. Figure 8.4 shows a comparison of single year-month statistics for a few U.S. locations where surface reports were available. The NASA cloud data are from the gridpoint nearest the ground location. U.S. locations were chosen for this comparison since satellite values tend to dominate U.S. portions of the data base.

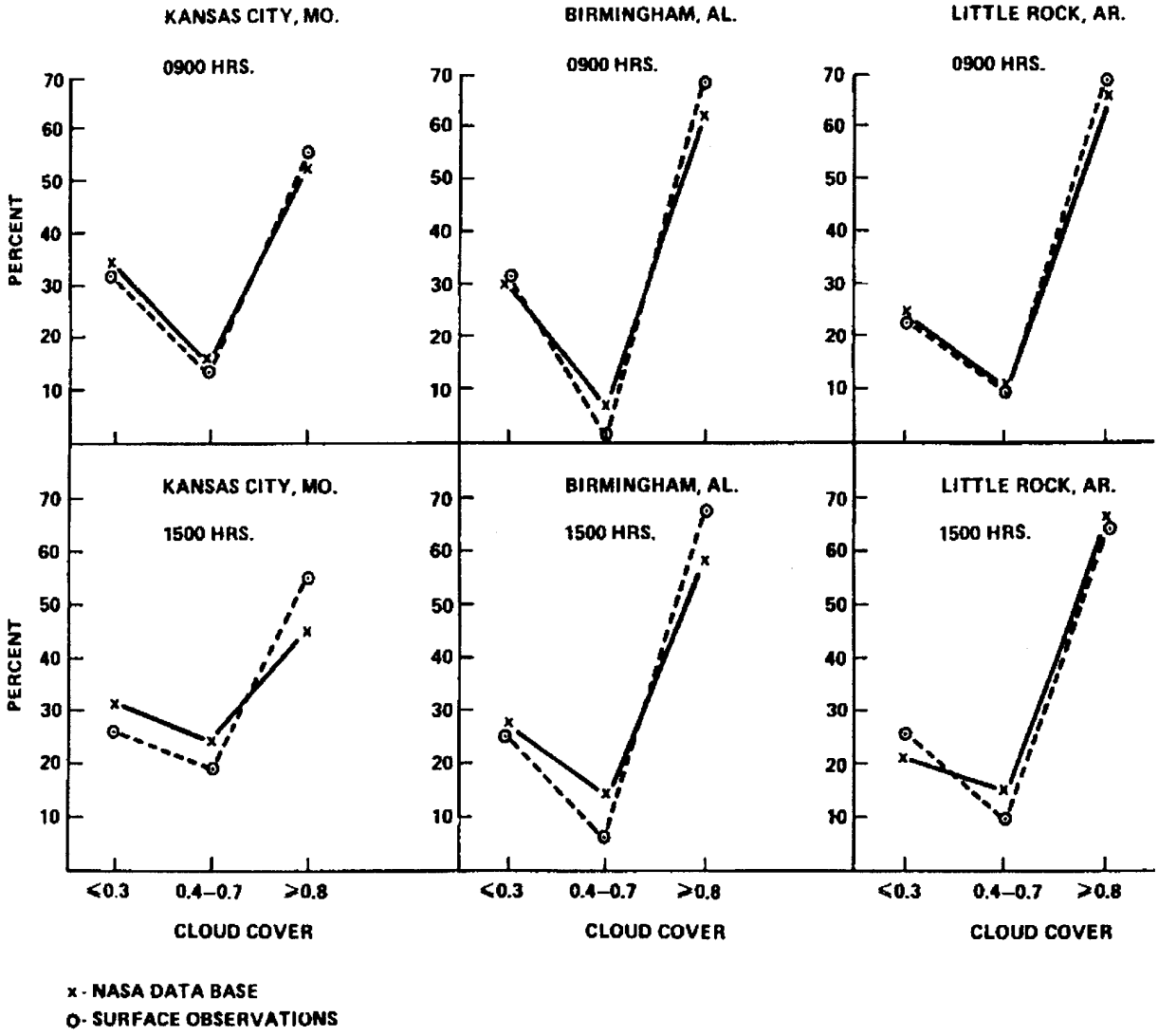

FIGURE 8.4 Cloud Cover Comparison – Surface Observations and Nasa Data Base, January 1973.

Table 8.1 shows cloud cover statistics calculated from the 5 years of this new data base compared with long term ground observed statistics extracted from the previous data base (Ref. 8.9).

As in the figure 8.4 case, the new statistics apply to the grid point closest to the ground station - in some cases they may be as much as 25 nmi apart. This geographic separation, especially in coastal or mountainous areas, might produce different cloud regimes at the two locations. Cloud amount differences can also be expected between the ground climatology versus satellite (NASA) observations and the different period of record of the two samples. Still, there is good agreement between the two data bases. For example, the percent frequency of ≥ 0.8 cloud cover at 1,500-h local time for the ground stations averaged 5-percent higher in winter and 10-percent higher in summer as seen in Table 8.1. Still other investigators have used different validation procedures to verify the basic 3D NEPH data (Refs. 8.11, 8.13, 8.14).

Figures 8.5 and 8.6 illustrate some hemispheric cloud cover values developed from this new data base. Both figures show a rather dramatic increase in NH cloudiness in 1977. For that year, the mean NH cloud cover was 57 percent. January showed the minimum coverage (49 percent) and July the maximum (62 percent). All available months except mid-1975 were consistently much less for 1972 through 1975 in the NH, yielding a 5-year mean of 46 percent. Mean 1977 coverage for the SH was also 57 percent with the minimum in September (54 percent) and the maximum in February (63 percent). Except for the first two-thirds of 1976, all available months for 1976 through 1980 consistently varied within ±7 percent of this mean value in the SH, yielding a 5-year mean of 56 percent. In general, the data depict scattered conditions in the NH for the first half of the decade of the 70's with a possible trend toward broken conditions during the latter half. However, broken conditions prevail in the SH over the entire last half of the decade.

Large variations were observed in the 1975–76 data, attributable in part to modifications in the automated analysis program. However, such variations scarcely negate the usefulness of this new data base for certain purposes since earlier NH data exhibit strong internal consistency, as does later SH data.

Furthermore, it should be remarked that the 3-D NEPH data were derived from a program which had one major objective; i.e., producing operationally significant, Earth-orbital viewing data in a quasi-real-time mode. The program's continual thrust was toward greater and greater clarity of such satellite-derived data. Minimal consideration was necessarily given to possible variations between past, current, and future data except as they impacted client missions. In short, as those who have ever been involved in such efforts are fully aware, "yesterday" is passe, "today" is paramount, and "tomorrow" is problematical though being planned. Archival of data was essentially undertaken in acknowledgment of the waste of data destruction and because such action was only minimally more troublesome or costly than any destruction.

This effort was only one of several which were undertaken in an attempt to revitalize the usefulness of these archived data. Naturally, because of its nature, discrepancies in the 3-D NEPH archive are to be expected. Future investigations of these variations are planned; but, as others have suggested, the 3-D NEPH data is probably the best of its kind currently available (Refs. 8.14, 8.15).

8.3.4 The Earth-Viewing Simulation Procedure. The great attribute of this data base in Earth viewing applications is the direct use of observed cloud cover instead of a Monte Carlo selected cloud amount. This is especially advantageous when the Earth target area is larger than the area viewed by the sensing instrument. For example, suppose the desired target area is 1,000 x 100 nmi and a camera acquires a series of pictures 100 x 100 nmi which are pieced together to cover the desired area. To simulate this situation using a statistical cloud cover data base requires a Monte Carlo draw of cloud cover encountered in the initial 100 x100 nmi picture. This first part is a reasonable approach which should give good results for the first picture. For the remainder of the 1,000 nmi swath, however, the Monte Carlo procedure becomes more complicated and less likely to produce reasonable results—due to the spatial (and sometimes temporal) continuity of clouds. To avoid unreasonable cloud patterns such as alternating clear and overcast in the remaining nine 100 x 100 nmi squares, the statistical data base must have additional time and space conditional probability distributions - which induces a further departure from reality.

Table 8.1 Comparison of climatology with NASA data base.

Probability of ≤0.3 and ≥0.8 cloud cover at 0900 and 1500 hours in December and July.

Station	December								July							
	≤0.3				≥0.8				≤0.3				≥0.8			
	0900		1500		0900		1500		0900		1500		0900		1500	
	C	N	C	N	C	N	C	N	C	N	C	N	C	N	C	N
Dhahran, Saudia Arabia	0.49	0.37	0.53	0.36	0.22	0.32	0.25	0.28	0.81	0.83	0.84	0.85	0.09	0.01	0.07	0.00
Tripoli, Libya	0.38	0.28	0.33	0.29	0.35	0.35	0.35	0.36	0.89	0.74	0.91	0.83	0.02	0.03	0.03	0.00
Angeles, Luzon, P.I.	0.16	0.13	0.10	0.02	0.58	0.55	0.60	0.59	0.01	0.01	0.01	0.00	0.76	0.74	0.80	0.80
Tampa, Florida	0.39	0.34	0.37	0.30	0.37	0.39	0.36	0.36	0.20	0.20	0.07	0.10	0.38	0.38	0.55	0.40
Mountain Home, Idaho	0.22	0.14	0.22	0.15	0.62	0.62	0.60	0.59	0.74	0.66	0.65	0.59	0.11	0.10	0.14	0.15
Fort Yukon, Alaska	0.31	0.48	0.34	0.41	0.55	0.29	0.54	0.39	0.28	0.27	0.21	0.38	0.48	0.37	0.43	0.28
Belleville, Illinois	0.29	0.21	0.28	0.23	0.57	0.65	0.58	0.60	0.31	0.46	0.25	0.31	0.41	0.32	0.36	0.25
Ban Me Thuot, Vietnam	0.07	0.30	0.14	0.26	0.40	0.44	0.36	0.44	0.03	0.26	0.00	0.28	0.51	0.47	0.51	0.38
Ship D (Atlantic)	0.13	0.06	0.04	0.04	0.60	0.67	0.68	0.73	0.15	0.32	0.15	0.35	0.61	0.35	0.55	0.32
Adak, Alaska	0.04	0.02	0.03	0.03	0.71	0.69	0.71	0.73	0.02	0.01	0.03	0.02	0.84	0.87	0.80	0.83
Resolute, NWT, Canada	0.64	0.65	0.50	0.61	0.31	0.08	0.37	0.15	0.20	0.12	0.17	0.13	0.64	0.38	0.66	0.45
Fort Kobbe, Canal Zone	0.26	0.28	0.16	0.10	0.37	0.27	0.48	0.30	0.03	0.00	0.00	0.01	0.80	0.67	0.82	0.70
Bangalore, India	0.30	0.47	0.26	0.45	0.31	0.18	0.34	0.17	0.00	0.01	0.00	0.06	0.80	0.79	0.77	0.67
San Francisco, California	0.32	0.24	0.39	0.26	0.55	0.41	0.46	0.41	0.72	0.35	0.84	0.50	0.16	0.23	0.08	0.18
Shreveport, Louisiana	0.33	0.32	0.36	0.38	0.53	0.51	0.48	0.46	0.34	0.30	0.27	0.27	0.33	0.34	0.34	0.26
Ship V (Pacific)	0.17	0.35	0.18	0.32	0.54	0.32	0.53	0.34	0.16	0.39	0.25	0.48	0.56	0.30	0.52	0.25

C = Climatology N = NASA

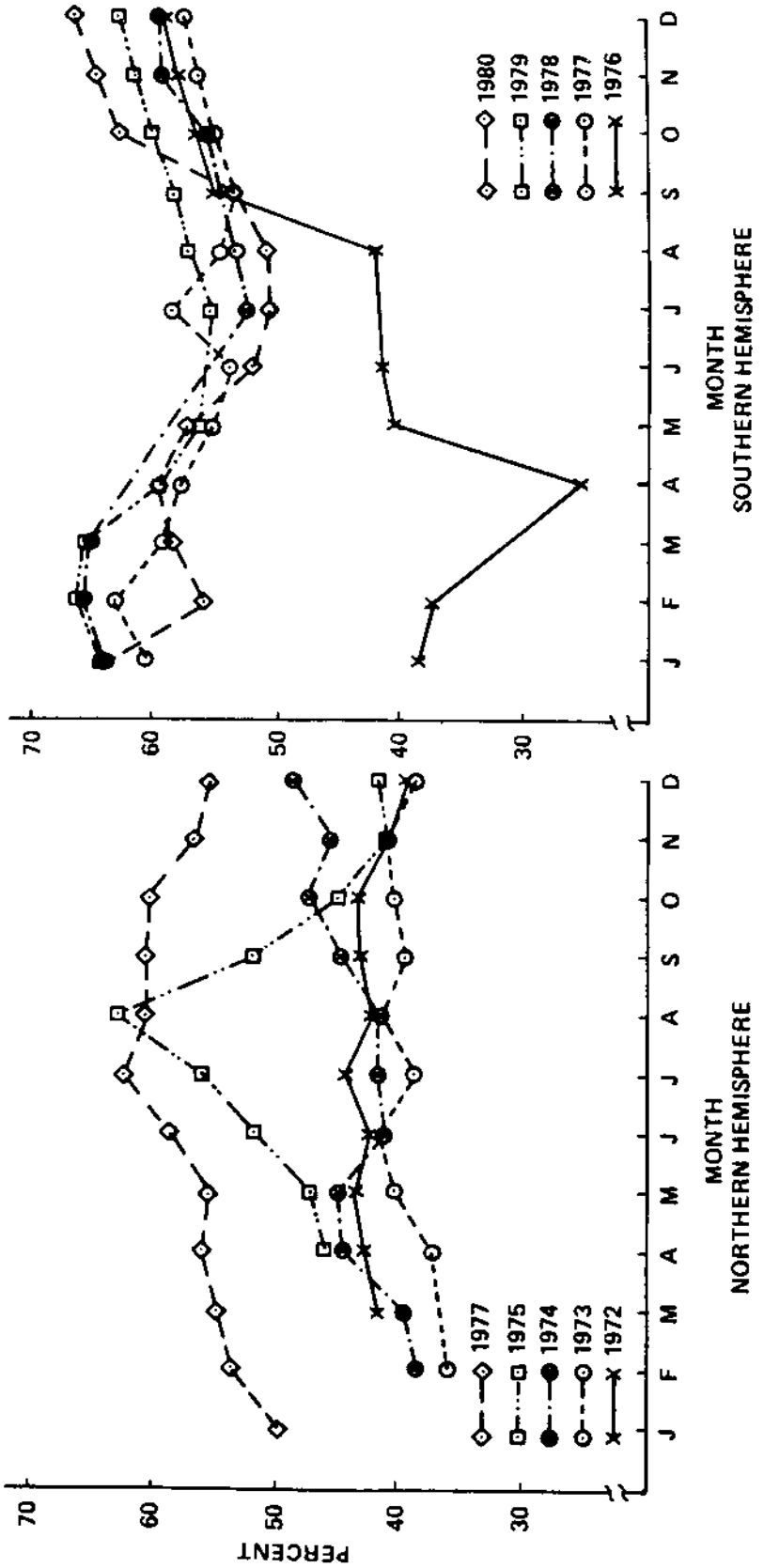

Figure 8.5 Mean hemispheric cloud cover.

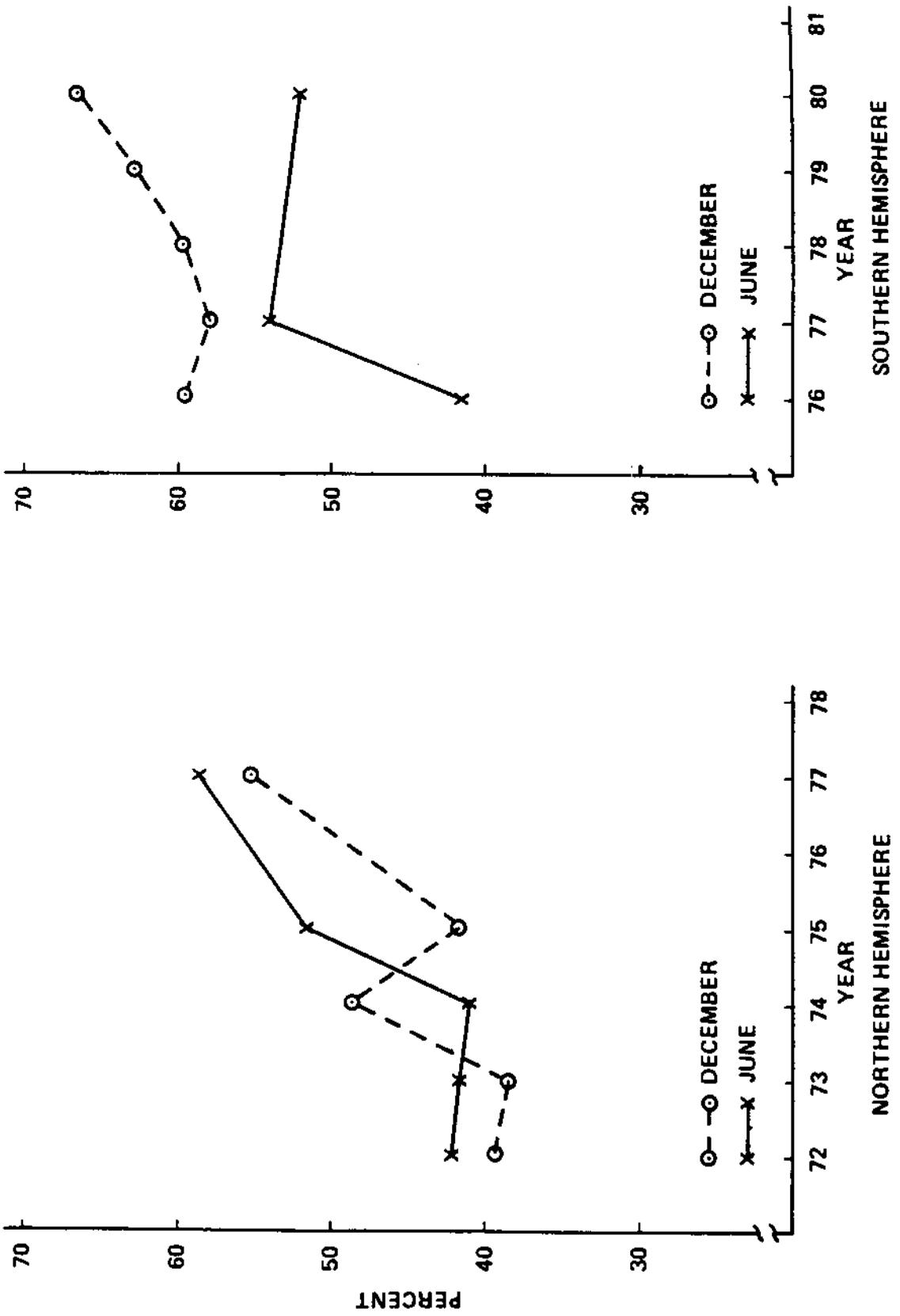

Figure 8.6 Mean monthly cloud cover.

Earth viewing simulations, using the new data base, bypass the time and space conditional probability problem by always using observed cloud cover. Although no missions have yet been analyzed with this NASA data base, the mechanics of the simulation procedure have been developed along with an ephemeris program and a program to locate gridpoints from latitude/longitude coordinates.

To illustrate the simulation procedure, consider, for example, the case described above where it is required to photograph a swath 1,000 nmi long and 100 nmi wide.

(1) Step 1—Locate the gridpoint closest to the center of the first 100 x 100 nmi square and the four surrounding gridpoints; i.e., I+1, I-1, J+1, J-1.

(2) Step 2—Calculate the mean cloud cover of those five points for the appropriate date/time and assign that value to the first square.

(3) Step 3—Move 100 nmi along the ground track and repeat step 1 and step 2. Repeat until all ten 100 nmi squares have an assigned cloud cover.

(4) Step 4—Average the ten values from above to obtain a single cloud cover for the entire swath. One minus the cloud cover is the fraction of Earth viewed on the first pass or revolution over the target area. Store this value.

(5) Step 5—Repeat the entire process the number of times in the month or season the actual mission will be flown.

(6) Step 6—Summarize the results to show: (a) The probability of success (where success is defined as photographing some specified percent of the swath) versus number of satellite passes over the target (Fig. 8.7). (b) Probability versus area photographed for a specified number of satellite passes over the target (Fig. 8.8).

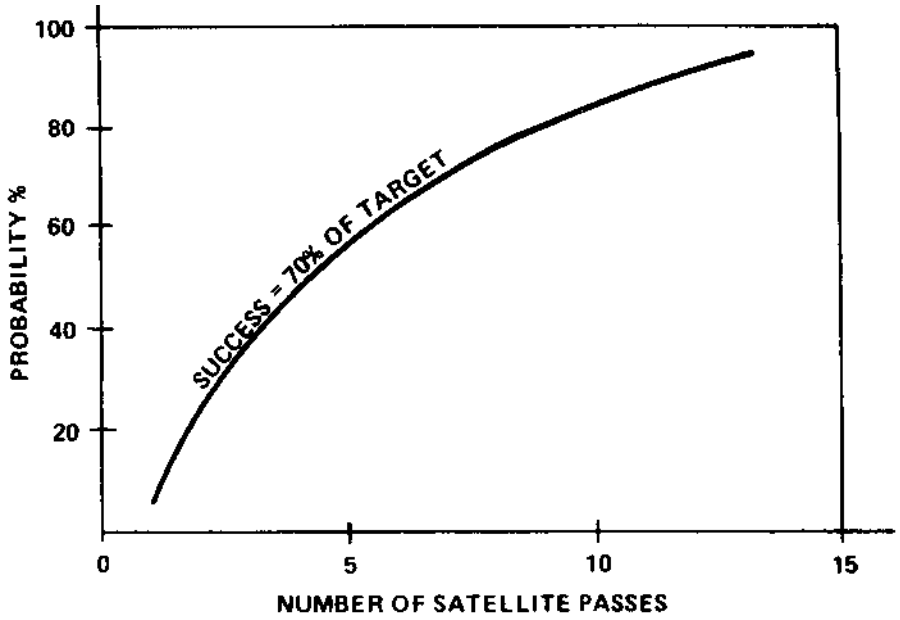

FIGURE 8.7 Probability of Success.

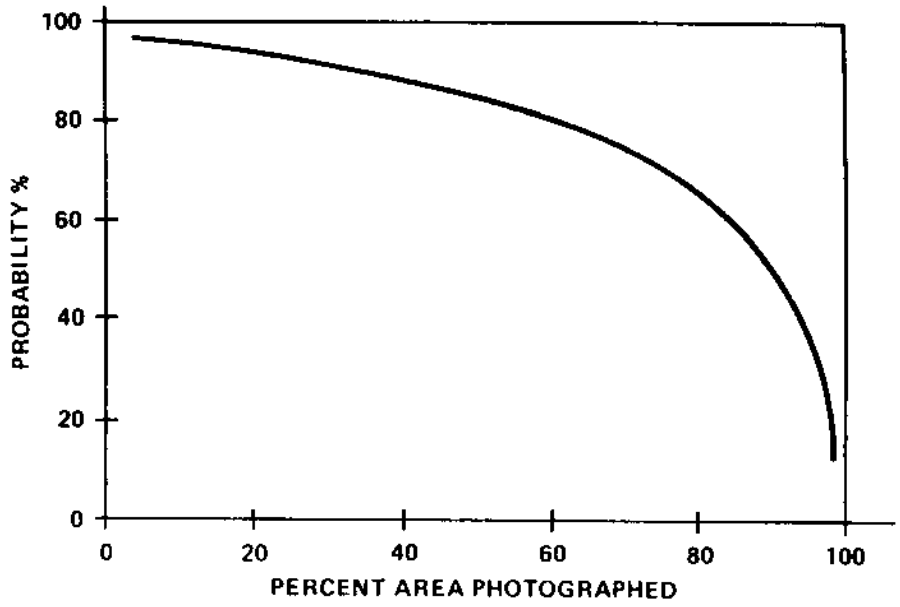

FIGURE 8.8 Photographic Coverage of Target Area After 10 Satellite Passes.

While the example specified a 1,000 x 100 nmi swath, the simulation procedure can be applied to any size area from a single grid point to a continent. Also, details as fine as single grid points within larger areas can be analyzed. For example, perhaps the mission requirements can be satisfied by incremental photographic coverage, i.e., forming a montage from parts of the area acquired on separate satellite revolutions, rather than acquiring the necessary amount on a single try. In this case, single grid points within the area can be cleared on successive passes to contribute to the area coverage. There is enough built-in flexibility to accommodate a wide variety of mission requirements.

8.4 Four-Dimensional Atmospheric Models. In this part of the attenuation model project, the emphasis is placed on water vapor rather than clouds. Also, since attenuation calculations are usually made from reference atmosphere inputs, the other atmospheric parameters found in reference atmospheres were included in the MSFC 4-D model. The basic data comprise monthly statistics (mean and standard deviations) of pressure, temperature, density, and moisture content from 0- to 25-km altitude on a global grid network. These data provide information on latitudinal, longitudinal, altitudinal, and temporal variations of the parameters; hence the name “four-dimensional atmospheric models.” Of course, a profile of temperature, pressure, density, and moisture content for any global location may be retrieved from these data. Still, to reduce the data to a more manageable amount it was decided to outline homogeneous moisture content regions for which a single set of profile statistics would apply. This procedure would permit the use of one set of profiles for all locations within a homogeneous region. For each region, analytical functions have been fitted to the statistical data. For moisture, exponential functions were most appropriate, while for temperature, a series expansion technique was used. Fitting analytic functions to the statistical climatological profile data produces a library of coefficients for the temperature and moisture profiles. These coefficients are then used to develop computer subroutines to regenerate the model profiles of temperature and moisture which are a function of the homogeneous region and month of the year.

In the compilation of the global statistics, pressure and density were determined from the hypsometric equation and the equation of state, rather than linear or logarithmic interpolation. The purpose of this was to insure hydrostatic consistency; thus, the pressure and density profiles can be generated from the temperature profile and the hydrostatic assumption.

The final result of this 4-D model analysis is a computer program that provides mean and variance profiles of moisture, temperature, pressure, and density from the surface to 25-km altitude for any location on the globe and month of the year. The computer program contains the equations, data, and library of coefficients necessary to produce the desired results. The thermodynamic parameters from this model were subsequently used to produce the lower segment (0- to 25-km altitude) for the Global Reference Atmosphere Model, 1990 (GRAM-90) (Ref. 8.16). However the GRAM-90 does not output any moisture parameters. The MSFC 4-D atmospheric model is described in references 8.4 and 8.5.

8.5 Stratospheric and Mesospheric Clouds. Four types of high-altitude clouds are presented in this subsection to alert designers and planners to the fact that there exists cloud systems/particles above the troposphere which need to be considered when observations or vehicle reentry, launch or horizontal flight above 12-km altitude is desired. Two related types of stratospheric cloud phenomena are presented here which occur at stratospheric altitudes (15 to 30 km) and are called polar stratospheric clouds (PSC), and nacreous clouds (NAC). Two similar types of upper mesospheric clouds (80- to 85-km altitude) called polar mesospheric clouds (PMC) and noctilucent clouds (NLC) will also be discussed briefly. The polar stratospheric clouds can be frozen aerosol particles, whereas the mesospheric clouds consist mainly of water ice. A global tropospheric cloud cover model is described in paragraph 8.3. See section 10 for more information on atmospheric constituents, aerosols, and chemistry.

8.5.1 Stratospheric Clouds

8.5.1.1 Polar Stratospheric Clouds. Polar stratospheric clouds were discovered in the late 1970's when they were observed as extinction amounts in the SAM II and LIMS satellite data (Ref. 8.17). They are probably not the visually observed nacreous clouds, but nacreous is a special subset of PSC's (Ref. 8.18). They appear not to be related to orographic features and appear larger and more persistent than nacreous clouds, PSC's may not even be visible to the ground observer. Therefore these high extinction stratospheric layers (aerosol related) were named polar stratospheric clouds (Ref. 8.17 and 8.19).

Polar stratospheric clouds are frozen aerosol particles observed in local winter over both polar regions whenever the ambient temperature falls below about 195 K. On one occasion they were observed extending continuously from 80° N. to the pole. The clouds are layered with the maximum amount near 20 km, close to the region of minimum stratospheric temperature. The layers are thin; <1 to 2 or more km thick (thicker in the Antarctic) in the altitude range from 10 to 30 km. Multiple layers of PSC's can exist. PSC's descend in altitude during the course of the winter until they reach an altitude of about 15 kms at the end of the winter. Antarctic PSC's generally occur at lower altitudes (<17 km) than Arctic PSC's (17 to 25 km). PSC's are also linked to the ozone depletion/hole over the poles (Ref. 8.25). This is in agreement with the predicted mean flow in the polar vortex. This results in a strong gradient across the polar night jet stream which lasts until the springtime breakup. This feature is in good agreement with the observed aerosol properties. The cloud characteristics change rapidly, most probably due to fluctuations in local temperature, water vapor, or wind shear. The clouds are apparently formed from frozen nuclei consisting primarily of either a nitric acid mixture (type I), or water ice particles (type II). Small admixtures of other compounds such as sulfuric and hydrochloric acid in solid solution also can exist with these two mixtures in the formations of PSC's (Ref. 8.20). The clouds are much more prevalent in the Antarctic with their colder (by 3.5 K) stratospheric temperatures than they are in the Arctic. If they were illuminated, these polar stratospheric clouds would have the appearance of a thin cirrus or cirrostratus

veil. The clouds are not formed at the level of maximum aerosol concentration but near the level of minimum temperature. References 8.17 through 8.24 describe polar stratospheric clouds and their characteristics. Although different kinds of polar stratospheric clouds exist which may have different compositions, they exist as highly supercooled/supersaturated liquid drops.

8.5.1.2 Polar Stratospheric Clouds (PSC) Design Criteria (1).

	PSC Type IPSC		Type II
Composition/phase	HNO_3 (2)/Ice		H_2O/Ice
Concentration	2 cm^{-3}		0.03 cm^{-3}
General Range	1 to 10 cm^{-3} (at 20 km)		0.005 to 0.1 cm^{-3} (at 15 km)
Mass Density	20 ppbm*		400 ppbm
Radius	0.5 μm		≥ 6 μm
Range		0.1 to 10 μm	
Temperature	<195 K		<195 K
	Antarctic		Arctic
Altitude	15 km		20 km
Range	11 to 22 km		17 to 25 km
Time of Occurrence	June to October		December to March
Associated Stratospheric Water Vapor Content: Avg		7 ppmv*	
Upper Limit	15.5 ppmv		21.5 ppmv
Horizontal Extent		10 to 10^3 km	
Geographic Extent		from 70° to Pole	
Duration		Hours to Months	

(1.) Much is based on Ref. 8.24.
(2.) Nitric acid mixture, >40-percent concentration
*ppbm = parts per billion mass and ppmv = parts per million volume.

8.5.1.3. Nacreous Clouds. Nacreous clouds, also called “mother-of-pearl clouds” (MPC), luminous clouds, or stratospheric veil clouds are infrequently observed, thin stratospheric clouds appearing brilliantly colored and stationary (lenticular) in wintertime over high latitudes in both hemispheres, i.e., Scandinavia, Alaska and Antarctica, when the Sun is below the horizon. Over 155 dates in which northern hemispheric sightings (for undisturbed stratosphere only, no aircraft contrails included), of NAC’s have

been observed over 100 years during winter (December to February). Somewhat more frequent are NAC's over the Antarctic winter (June to September) where over 140 sightings in 100 years have occurred in these sparse reporting areas (Ref. 8.26). NAC's have been sighted between 17- to 31-km altitude (average 23 km), and set-up preferentially downwind of mountain ranges. This indicates orographic origin with lee waves producing up to 40-km wavelengths present in the NAC bands. NAC's are a special subset of polar stratospheric clouds, but it is not yet clear that the two-cloud phenomena are the same (Ref. 8.18). NAC's are composed of micrometer-sized water ice particles (crystals) with sizes of the order of 1 to 2 μm in radius, and life times are >10 min at 20 km, 1 ppm of water is equivalent to 5 particles cm^{-3} of size 1.5 μm. An approximate maximum radius of about 4 μm at 20 km altitude may be determined, assuming 3 ppm of water condensing to form 1 particle cm^{-3}. It is generally believed that NAC's form by deposition of H_2O on pre-existing stratospheric aerosol particles (sulfate), when stratospheric temperatures are typically at or below –85 °C. Therefore, the number concentration of NAC particles should be equal to that of the stratospheric aerosols (~5 to 20 cm^{-3} at 20 km).

8.5.2 Mesospheric Clouds. Mesospheric clouds fall into two separate, but similar, cloud (water ice) phenomena that occur at cold, summertime, high latitude mesopause altitudes. Such phenomena are known as noctilucent clouds in their twilight manifestation between 50° and 65° latitude, via ground based observations; and as polar mesospheric clouds in their extension into the entire polar/daytime regions (65° to 85° latitude, with some occurrences as low as 55° latitude). PMC's are believed to be the brighter extension of NLC's into the northern and southern polar cap region. Both phenomena are similar and keyed to the summer solstice when temperatures fall below 140 K at mesopause heights. This suggests that variations of temperature and/or the accompanying upward advective water vapor flux are responsible for the seasonal variations of PMC and NLC (Ref. 8.27).

8.5.2.1 Polar Mesospheric Clouds. PMC's are scattering layers observed by satellite that occur at high latitude, summertime, mesopause regions over extensive areas of both poles. PMC's develop at the coldest point over the planet as small ice particles grow by sublimation on available nuclei. Nucleation upon meteoric dust (or condensed vapor) and/or hydrated ions has been investigated and both routes are plausible (Ref. 8.28).

8.5.2.2 PMC Seasonal Climatology. Comparison of PMC seasonal properties for 1981–1985 with NLC (1885–1972). Times are given in days after summer solstice (Ref. 8.27).

	South PMC	North PMC	North NLC
Beginning date[1]	–32	–23	–38
Ending date	61	64	50
Time of maximum	7–16	16–22	16–20
Duration of season	93	87	88
Lower latitude boundary	65° (PM)[2]	60° (PM)[3]	45° N./50° S.
Months observed		June–August	
Interannual variability	±15 percent	±15 percent	
Altitude, km	83.2±1.5	85.0±1.5	

1. Begins at high latitude 10 to 20 days before lower latitude observation. South Pole seasonbegins earlier
2. 55° (AM)
3. 60° (AM)

8.5.2.3 PMC Properties.

Ice particle size: 35- to 70-nm range

Ice particle concentration: 190 cm^{-3} (5- to 500-cm^{-3} range)

Ice particle column number: 10^6- to 10^8-cm^{-2} range

Water mixing ration (w): 1 to 4 ppmv

Temperature: <140 K

Cloud thickness: 2 to 3 km

Cloud extent: 100 x 100 km.

8.5.2.4 Noctilucent Clouds

8.5.2.4.1 Background. Noctilucent clouds were once thought to be very rare, especially in the Southern Hemisphere; however, observations from space have shown that they occur almost continuously during some periods of time. In both hemispheres their coverage can be quite extensive. Noctilucent clouds are composed of submicro- sized water ice particles growing in supersaturated air and occurring in a few-kilometer thick layer, only during summer over higher latitudes (poleward of 45° N. and 50° S.) at cold (<140 K) mesopause altitudes (85 km). These clouds have been observed only from the ground over the past 100 years, at twilight (morning or evening) when the Sun is between 6° and 16° below the horizon, so that the 80- to 85-km level is still in sunlight. Whether NLC and PMC both represent the same phenomenon currently remains an open question. The exact relationship between NLC and PMC is not yet known (Ref. 8.28). The NLC season begins and ends much earlier than PMC, and occurs at significantly lower latitudes than do PMC. Jensen and Thomas have stated that they feel PMC and NLC could actually be the same phenomenon with their cloud property differences noted, being due to their variation with local time, since the two phenomena are observed at different diurnal times. The following was extracted from references 8.27, 8.29, 8.30, and 8.31.

8.5.2.4.2 Types. Fogle and Haurwitz (Ref. 8.31) have classified noctilucent clouds as follows:

TYPE I. VEILS—These are the simplest. They are very tenuous with no well-defined structure, and are often present as a background for other categories or forms. They are somewhat like cirrus clouds of uncertain shape; however, occasionally they exhibit a faintly visible fibrous structure. They often flicker.

TYPE II. BANDS—These are long streaks with diffuse edges (type IIa) or sharply defined edges (type IIb). They are sometimes hundreds of kilometers long and often occur in groups arranged roughly parallel to each other or interwoven at small angles (perhaps visible evidence of the gravity waves propagating through the region). Occasionally an isolated band is observed. Bands change very little with time and blurred bands with little movement are often the predominant structure in the noctilucent cloud field. When they do move, it is often in a direction and with a speed that is different than that of the display as a whole. Very closely spaced thin streaks, called serrations, are occasionally seen in the veil background. They look like a continuous cloud mass since the serrations are separated by only a few kilometers.

TYPE III. BILLOWS—These are groups of closely spaced short bands which sometime consist of straight and narrow, sharply outlined parallel short bands (type IIIa). Sometimes they exhibit a wave-like structure (type IIIb). The distance separating pairs of billows is about 10 km. Billows sometimes lie across the direction of the long bands and their alignment usually differs noticeably in close portions of the sky. Unlike the long bands billows may change their form and arrangement or even appear and disappear within a few minutes.

TYPE IV. WHIRLS—Whirls of varying degrees of curvature are also observed in veils, bands, and billows; infrequently, complete rings with dark centers are formed. Whirls of small curvature (less than 1.0°) are classified as type IVa while whirls having a single simple band or several bands with a radius of 3° to 5° are classified as type IVb. Larger scale whirls are classified as type IVc.

TYPE V. AMORPHOUS—These are similar to veils in that they have no well-defined structure but they are brighter and more readily visible than the veil type NLC.

8.5.2.4.3 Characteristics. Typical characteristics of NLC based on ground-based observations in the Northern Hemisphere are given in the following from Fogle and Haurwitz (Ref. 8.31) and references 8.27, 8.29, and 8.30:

Color	Bluish-white
Height (average)	82.7 km, maximum 95, minimum 73
Latitude of observations	45 to 80°; best about 60°
Season of observation	Northern Hemisphere: March through October, best June through August Southern Hemisphere: December through January
Time	While the solar depression angle varies from 6° to 16°
Spatial extent	10^4 to more than 4 x 10^7 km^2; can cover considerable parts of latitudinal belts north of 45°
Duration	Several minutes to more than 5 hours
Average velocity	40 m s^{-1} towards the southwest. Individual bands often move in different directions and at speeds differing from the NLC display as a whole.
Thickness in the vertical	0.5 to 2.0 km
Vertical wave amplitude	1.5 to 3.0 km
Average particle diameter	$3x10^{-5}$ cm
Particle number density	10^{-2} to 1/cm^3
Ambient temperature when NLC present	135 K
Brightness	<0.4 candles/cm^3
Albedo	$2.3x10^{-5}$ to $4.7x10^{-5}$
Polarization	Strongly polarized in same sense as, but less sharply than twilight sky.

8.5.2.4.4 Particle Size and Number Density. It is generally agreed that noctilucent clouds consist of ice particles; however, there is disagreement as to whether or not they are aligned or randomly oriented. There is general agreement that they consist principally of particles of a radius of 0.1 to 0.2 μm; however, there is evidence to indicate that some particles may be larger than 1 μm in radius. Number densities range from 10^{-2} to 1 cm^{-3}. The particle size distribution is given by the Junge law (Ref. 8.29):

$$dn(r) = c \times r^{-v}\, d(\ln r) \tag{8.1}$$

where r is the radius, c is a measure of the turbidity depending upon the density per cubic centimeter, and $2<v<3$.

8.5.2.4.5 Composition. There is disagreement as to what the growth mechanism is, condensation or coagulation; however, there is agreement that supersaturated conditions can be expected to occur at the mesopause in the summer hemisphere. The question still remains as to whether or not there is enough moisture to generate the amount of clouds observed. Figure 8.9 shows the water vapor content of the atmosphere to an altitude of 100 km. Observations show that nickel, iron, carbon, copper, etc. are present in the nuclei. These are possibly of extraterrestrial origin. There is further evidence to support the concept that the nuclei could be ion clusters.

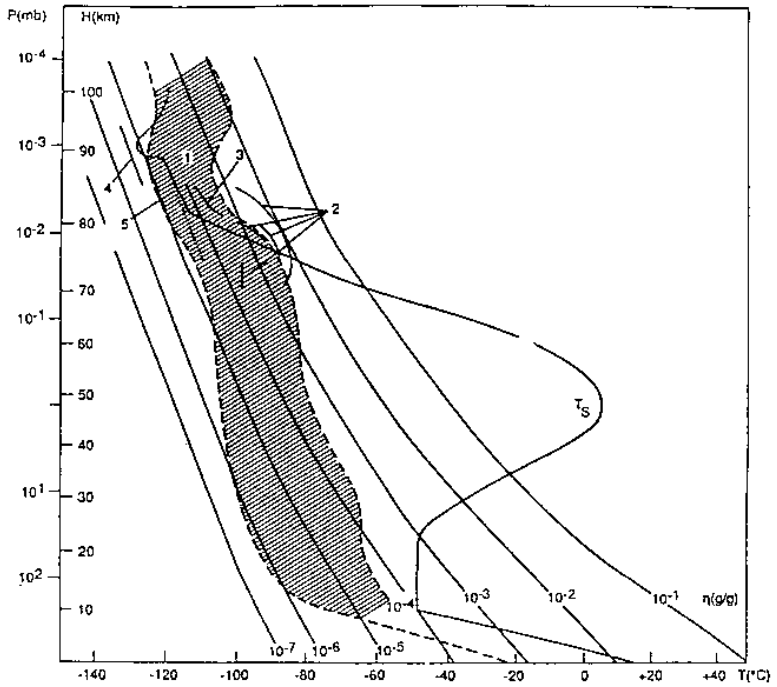

FIGURE 8.9 Water Vapor Mixing Ratio Versus Altitude: Data Generalized by (1) Sonntag, 1974, (2) Measurements by Perov and Fedynsky, 1968; (3) by Chyzhov and Kim, 1970; (4) by Arnold and Krankovsky, 1977; and (5) by Quessette, 1968. Curve T_S Gives the Mean Temperature at 60° N. in July by Cole and Kantor, 1978. Also Ascending Smooth Mixing Curves from 10^{-1} through 10^{-7} are Plotted.

8.5.2.4.6 Optical Properties. Results of analyses to date indicate that the optical thickness in the 0.2 to 0.4 μm wavelength interval can be approximated by:

$$t\,l = t\,l_0 \times 5.5\ l^{0.6} \exp(-2\ l^{0.65}) \qquad (8.2)$$

where $l_0 = 0.55$ μm.

REFERENCES

Section 8

8.1 Gaut, N.E., and Reifenstein, E.C., III: "Interaction Model of Microwave Energy and Atmospheric Variables." Environmental Research and Technology, Inc., final report of contract NAS8-26275, February 1971.

8.2 Sherr, P.E., et al.: "World Wide Cloud Cover Distribution for Use in Computer Simulations." Allied Research Associates, NASA CR-61226, June 14, 1968.

8.3 Greaves, J.R., et al.: "Development of a Global Cloud Model for Simulating Earth-Viewing Space Missions." Allied Research Associates, final report of contract NAS8-25812, January 1971.

8.4 Spiegler, D.B., and Greaves, J.R.: "Development of Four-Dimensional Atmospheric Models (World-wide)." Allied Research Associates, Inc., NASA CR-61362, August 1971.

8.5 Spiegler, D.B., and Fowler, M.G.: "Four-Dimensional Worldwide Atmospheric Models (Surface to 25-km Altitudes)." Allied Research Associates, Inc., NASA CR-2082, July 1972.

8.6 Brown, S.C., and Jeffries, W.R., III: "A New NASA/MSFC Mission Analysis Global Cloud Cover Data Base." NASA TR-2448, March 1985.

8.7 Coburn, A.R.: "Improved Three-Dimensional Nephanalysis." U.S. Air Force Global Weather Center, AFGWC Technical Memorandum 71-2, 1971.

8.8 Fye, F.K.: "The AFGWC Automated Cloud Analysis Model." U.S. Air Force Global Weather Center, AFGWC Technical Memorandum 78-002, 1978.

8.9 Anonymous: "VISSR Digital Archive User's Guide." National Climatic Center, Satellite Data Services Division, Applications Branch, 1978.

8.10 Kidwell, K.B.: "NOAA Polar Orbiter Data (TIROS-N) User's Guide (Preliminary Version)." National Climatic Center, Satellite Data Services Division, 1979.

8.11 d'Entremont, R.P., Hawkins, R.S., and Bunting, J.T.: "Evaluation of Automated Imagery Analysis Algorithms for Use in the Three-Dimensional Nephanalysis Model at AFGWC." AFGL Technical Report 82-0397, 1982.

8.12 Davis, P.A., and Wolf, D.E.: "Specifications of Cloud Cover Using Multispectral Satellite Radiometry Data." U.S. Dept. of Commerce Final Report PB-281160, 1978.

8.13 Henderson-Sellers, A., Hughes, N.A., and Wilson, M.: "Cloud Cover Archiving on a Global Scale: A Discussion of Principles." Bull. Am. Meteorol. Soc., vol. 62, 1981, pp. 1300–1307.

8.14 Hughes, N.A., and Henderson-Sellers, A.: "A Preliminary Global Oceanic Cloud Climatology From Satellite Albedo Observations." Jour. of Geophys. Res., vol. 88, C2, 1983, pp. 1475–1483.

8.15 Gordon, A., and Hovanec, R.: "The Sensitivity of Model-Derived Radiation Fluxes to the Monthly Mean Specification of Cloudiness." Clouds in Climate, Goddard Institute for Space Studies, NASA, 1981.

8.16 Justus, C.G., Alyea, F.N., Cunnold, D.M., Jeffries, W.R., III, and Johnson, D.L.: "The NASA/MSFC Global Reference Atmospheric Model—1990 Version (GRAM-90), Part 1: Technical/Users Manual." NASA TM-4268, April 1991.

8.17 Farrukh, U.O.: "Polar Stratospheric Cloud Sightings by SAM II: 1978–1982." NASA CR-177995, March 1986.

8.18 McCormick, M.P., and Hamill, P.: "Characteristics of Polar Stratospheric Clouds as Observed by SAM II, SAGE, and Lidar." Jour. Meteor. Soc. of Japan, vol. 63, No. 2, April 1985, pp. 267–276.

8.19 Hamill, P., and McMaster, L.R.: "Polar Stratospheric Clouds—Their Role in Atmospheric Processes." NASA CP-2318, 1984.

8.20 Hamill, P., Turco, R.P., and Toon, O.B.: "On the Growth of Nitric and Sulfuric Acid Aerosol Particles Under Stratospheric Conditions." JAC, vol. 7, 1988, pp. 287–315.

8.21 McCormick, M.P., and Trepte, C.R.: "Polar Stratospheric Optical Depth Observed Between 1978 and 1985." JGR, vol. 92, No. D4, April 20, 1987, pp. 4297–4306.

8.22 Kent, G.S., Poole, L.R., and McCormick, M.P.: "Characteristics of Arctic Polar Stratospheric Clouds as Measured by Airborne Lidar." JAS, vol. 43, No. 20, October 15, 1986, pp. 2149–2161.

8.23 Steele, H.M., Hamill, P., McCormick, M.P., and Swissler, T.J.: "The Formation of Polar Stratospheric Clouds." JAS, vol. 40, August 1983, pp. 2055–2067.

8.24 Kinne S., et al.: "Measurements of Size and Composition of Particles in Polar Stratospheric Clouds From Infrared Solar Absorption Spectra." JGR, vol. 94, No. D14, November 30, 1989, pp. 16481-16491.

8.25 Hofmann, D.J., et al.: "Stratospheric Clouds and Ozone Depletion in the Arctic During January 1989." Nature, vol. 340, July 13, 1989, pp. 117–121.

8.26 Stanford, J.L., and Davis, J.S.: "A Century of Stratospheric Clouds Reports: 1870–1972." Bull. AMS, vol. 55, No. 3, March 1974.

8.27 Thomas, G.E., and Olivero, J.J.: "Climatology of Polar Mesospheric Clouds 2, Further Analysis of Solar Mesosphere Explorer Data." JGR, vol. 94, No. D12, October 20, 1989, pp. 14673–14681.

8.28 Jensen, E., and Thomas, G.E.: "On the Diurnal Variation of Noctilucent Clouds." JGR, vol. 94, No. D12, October 20, 1989, pp. 14693–14702.

8.29 Kaufman, J.W.: "Noctilucent Clouds." NASA-MSFC/ES42 preliminary report, January 1989.

8.30 Toon, O.B., and Farlow, N.H.: "Particles Above the Tropopause." Ann. Rev. Earth Planet Sci., vol. 9, 1981, pp. 19–58.

8.31 Fogle, B., and Haurwitz, B.: "Noctilucent Clouds." Space Science Reviews, vol. 6, No. 3, 1966, pp. 279–340.